Taylor & Francis
Taylor & Francis Group

Automatika

Journal for Control, Measurement, Electronics, Computing and Communications

ISSN: 0005-1144 (Print) 1848-3380 (Online) Journal homepage: http://www.tandfonline.com/loi/taut20

Physically sound model of a non-Foster negative capacitor

Boris Okorn, Silvio Hrabar & Igor Krois

To cite this article: Boris Okorn, Silvio Hrabar & Igor Krois (2017) Physically sound model of a non-Foster negative capacitor, Automatika, 58:2, 244-252, DOI: 10.1080/00051144.2017.1398211

To link to this article: https://doi.org/10.1080/00051144.2017.1398211

Published online: 01 Dec 2017.

AUTOMATIKA, 2017
VOL. 58, NO. 2, 244–252
https://doi.org/10.1080/00051144.2017.1398211

Taylor & Francis
Taylor & Francis Group

REGULAR PAPER

Physically sound model of a non-Foster negative capacitor

Boris Okorn[a], Silvio Hrabar[b] and Igor Krois[c]

[a]Department of Materials Physics, Ruđer Bošković Institute, Zagreb, Croatia; [b]Department of Wireless Communications, Faculty of Electrical Engineering and Computing, University of Zagreb, Zagreb, Croatia; [c]Department of Electronics, Microelectronics, Computer and Intelligent Systems, Faculty of Electrical Engineering and Computing, University of Zagreb, Zagreb, Croatia

ABSTRACT

In both engineering and physics communities, it is believed that approximation of a realistic non-Foster negative capacitor (within its operating bandwidth) with an ideal dispersionless negative capacitor is acceptable for practical purposes. However, the ideal negative capacitor is not causal and, therefore, not compatible with basic physics. Its use in the design process is misguiding since it often predicts entirely non-physical behaviour. Here, we show that a realistic negative capacitor can always be modelled as a dispersive voltage-controlled source, the internal impedance of which is an ordinary positive capacitor. This equivalent circuit clearly explains the origin of negative conductance that always accompanies negative capacitance, as well as the background physics of previously reported counter-intuitive phenomena in non-Foster metamaterials. Theoretical analysis was verified by simulations and measurements on an experimental low-frequency (100 Hz–25 kHz) negative capacitor demonstrator. Measurement results agreed well with theoretical predictions, showing that the proposed model is indeed physically sound.

ARTICLE HISTORY
Received 4 August 2017
Accepted 21 October 2017

KEYWORDS
ENZ; non-Foster; negative capacitor; causality; active metamaterials; metamaterials

Introduction

An ordinary (positive) capacitor (Figure 1(a)) is a basic circuit-element, the current $i_p(t)$ and voltage $v(t)$ of which are related by a very well-known equation:

$$i_p(t) = C_p \frac{\partial v(t)}{\partial t}. \quad (1)$$

Here, C_p ($C_p > 0$) stands for the capacitance. It is an inherent physical parameter, defined as a ratio of the charge and applied voltage. It is very important to notice that this, indeed very basic, definition assumes that C_p is a constant. The capacitance is entirely independent on the signal time-domain waveform $v(t)$. In other words, C_p is assumed to be a linear device that is dispersionless in the frequency domain. Of course, this assumption is valid only within a framework of a standard circuit-theory (the signal retardation along a physical capacitor modelled by (1) is neglected, i.e. the capacitor dimensions are much smaller than a wavelength). Furthermore, in standard convention, it is assumed that the current $i_p(t)$ flows into the positive terminal of C_p (thus, a positive capacitor behaves as a reactive load).

Formally, it is possible to change the sign of the capacitance and define a negative capacitor $C_n < 0$, $C_n = -C_p$ [1–3] (Figure 1(a)). By rearranging (1), one gets the relation between the voltage at the negative capacitor ($v(t)$) and the associated current flowing through it ($i_n(t)$):

$$i_n(t) = C_n \frac{\partial v(t)}{\partial t} = -|C_n| \frac{\partial v(t)}{\partial t} = -i_P(t). \quad (2)$$

Equation (2) shows that, during the increase of the voltage across a negative capacitor ($\partial v(t)/\partial t > 0$), the current actually *flows out* of the positive terminal (thus, $i_n(t) < 0$). This behaviour is just opposite to the familiar behaviour of a positive capacitor, in which the current flows into the positive terminal during the charging phase ($\partial v(t)/\partial t > 0$). Clearly, a negative capacitor behaves as a (reactive) *source*, i.e. it is inevitably an active device.

Due to its active nature, the negative capacitor violates Foster's reactance theorem [4,5] ($\partial X/\partial \omega > 0$ and $\partial B/\partial \omega > 0$) (Figure 1(b)). Here, X and B stand for the reactance and susceptance ($B = 1/X = \omega C$), ω being the angular frequency with $e^{j\omega t}$ time dependence assumed.

One may call the negative capacitor (and the negative inductor that can be defined in a way similar to (2)) a "non-Foster" element [1–3]. Practical realization of non-Foster elements that employ active electronic circuits (the so-called "Negative Impedance Converters", NIC) was proposed for the first time back in the 1950s [6]. These circuits mimic the behaviour of ideal non-Foster elements only within a finite bandwidth.

CONTACT Boris Okorn boris.okorn@irb.hr

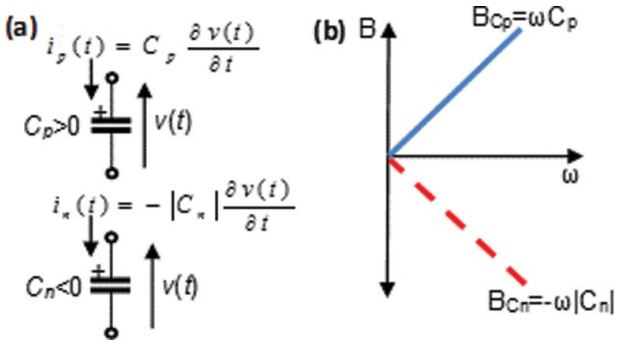

Figure 1. Positive capacitor (C_p) and negative capacitor (C_n). (a) Voltage and current convention (note that the current $i_n(t)$ is negative, and thus, it actually flows out from the positive terminal of C_n). (b) Susceptance of a positive (solid line) and a negative (dashed line) capacitor.

Strictly speaking, realistic non-Foster elements *cannot* be described by equation similar to (2) since it presumes dispersionless behaviour with infinite bandwidth. Although this fact is quite obvious, it is almost always neglected, both in engineering and physics communities.

An important potential application of non-Foster elements is in broadband electromagnetic devices. The basic idea relies on a compensation of the frequency dispersion of ordinary reactive (*LC*) network with the "inverse" dispersion of a "negative" non-Foster network [3], yielding (theoretically) infinite bandwidth.

Although the above idea was introduced more than 40 years ago [3], there are very few reports on the successful realization in the open literature. The reason for this lies in inherent instability of non-Foster elements [7–9]. Actually, most of the papers report solely theoretical results stating that practical realization is very challenging. Some successful implementations have been reported in the field of broadband matching of small antennas [7] and, very recently, in broadband active metamaterials [1,2]. The difficulties in practical realization led to a common opinion that the stability problem is associated with pure technological issues such as the occurrence of parasitic capacitances [10]. However, this is only partially true. We believe that the basic problems come from naive use of the standard circuit-theory with an ideal, dispersionless negative capacitor ($C_n < 0$). Unfortunately, this simple model is not causal (within framework of linear circuit and transmission line theory). In spite of this, many authors presume that the dispersion cannot affect the basic principles of associated application. As it will be shown later, this is entirely incorrect assumption.

This contribution proposes a causal, physically sound equivalent circuit (a model) of the realistic negative capacitor, which always predicts correct behaviour. The model is verified by measurements on a specially designed laboratory prototype, both in the time domain and the frequency domain.

Unclear issues in basic physics of a negative capacitor

There are studies that deal with a non-Foster element just as an ideal, dispersionless, positive element with a flipped sign (in the case of a capacitor, they use $C_n < 0$, $C_n = -C_p$), and then apply standard circuit-theory [11–14]. Strictly speaking, this approach, particularly common in theoretical studies, is (as it will be shown later) not correct. Occasionally, it may predict (qualitative) behaviour of a specific network but only in the steady-state conditions and only within some finite bandwidth. However, there are many cases, in which the behaviour predicted using a network that contains ideal non-dispersive negative elements is entirely non-physical. For instance, a long time ago, it was shown that a transmission line with an inserted ideal NIC should yield superluminal energy transport [15]. The same unphysical effect has been predicted recently [16] for a case of a transmission line terminated with a "negative image" of the characteristic impedance. Both studies [15,16] correctly emphasized that the cause of these obviously unphysical predictions lies in "the missing" link between stability and causality. A similar effect was further elaborated in [2,9], within a context of a transmission line periodically loaded with negative capacitors.

On the other hand, in most practical studies, authors start with the analysis of particular application based on ideal negative capacitance. Of course, all the authors are aware that every practical NIC has finite bandwidth and that generated negative capacitance will inevitably be dispersive. In spite of this, they incorrectly presume that the dispersion cannot affect the basic principles of associated application. Thus, they construct the NIC that should generate a negative capacitance equal to the capacitance in the ideal case. This tactic neglects the counter-intuitive physics of non-Foster elements and, unfortunately, very often leads to instability.

A rather striking example of counter-intuitive effects present in networks with ideal dispersionless negative capacitor is sketched in Figure 2(a). It depicts

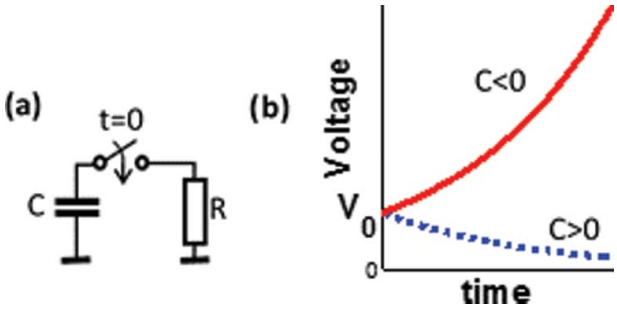

Figure 2. (a) Circuit with a charged capacitor connected abruptly to a resistor. (b) Voltage across the capacitor according to (3) (positive capacitor – dashed line; negative capacitor – solid line).

the discharging of an (initially charged) capacitor C by connecting it instantaneously to the resistor R [9]. It is well known from standard circuit theory that the voltage across the capacitor has exponential form:

$$v(t) = V_0 \cdot e^{-t/\tau}, \quad \tau = R \cdot C. \tag{3}$$

Here, V_0 stands for the initial voltage at the (charged) capacitor, t is the time and τ is the time constant. In the case of an ordinary (positive) capacitor, both R and C are positive numbers. Therefore, the time constant τ is a positive number, as well. This leads to a familiar exponential decay of the voltage (i.e. discharging of a capacitor) (dashed line in Figure 2(b)). However, in the case of a negative capacitor, the time constant τ is a negative number (due to $C < 0$) causing an unbounded exponential grow of the voltage (solid curve in Figure 2(b)). Therefore, the energy dissipated at the resistor ($\int [v(t)]^2 dt/R$) will (at some time instant) exceed the initial energy stored in the capacitor ($V_0{}^2C/2$). This effect seems to violate the energy conservation, pointing out a fact that a negative capacitor must be an active device (with an embedded energy source). Looking from a different point of view, the unbounded voltage growth is a signature of instability. Indeed, analysis of the natural response shows that there is a real pole in the right-hand side of the complex plane (located at $s = -1/(RC)$, s being the complex frequency, $s = \sigma + j\omega$). Where does this instability come from? Unfortunately, the clear explanation of physical origin of the instability that could help in practical design has not been reported yet.

The second example deals with a recently introduced ultra-broadband Epsilon-Near-Zero (ENZ) metamaterial [1,2]. It is based on a transmission line periodically loaded with negative capacitors at distances much shorter than the wavelength. It can be thought that a differential shunt branch of a loaded transmission line comprises a parallel combination of the line capacitance $C'\Delta x$, (C' and Δx being distributed capacitance and the segment length that is much shorter than a signal wavelength, respectively) and a negative capacitor C_n (Figure 3) [1].

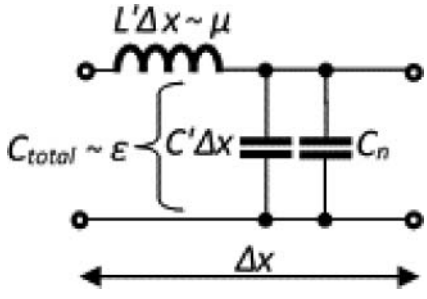

Figure 3. Equivalent circuit of a differential section of a transmission line periodically loaded with negative capacitors (1D ENZ metamaterial).

Thus, the overall capacitance is given by

$$C'\Delta x \| C_n = C'\Delta x + C_n = C'\Delta x - |C_n|. \tag{4}$$

Providing that $|C_n| < C'\Delta x$, the overall capacitance is lower than the original capacitance and the equivalent relative permittivity is lower than one ($\varepsilon_{reff} < 1$). According to (4), this ENZ effect is entirely dispersionless, i.e. it does not depend on the frequency at all. This would lead to the existence of superluminal energy propagation, which certainly violates causality. It was noticed [2] that a solution of this paradox lies in the fact that every realistic negative capacitor is always a frequency-limited device. Thus, the negative capacitance effect must cease at some frequency (for example, experimental study [1] reported very broad, but finite, bandwidth of 1:40). So, a simple (mathematical) capacitance "negation" (2) is not physically sound. Furthermore, a formal description of the capacitance decrease in (4) does not explain the background physics. Does the negative capacitor somehow decrease the charge in the shunt branch of a loaded transmission line and, therefore, alter the equivalent capacitance? If so, how does the negative capacitor influence the energy distribution in the system? The answers to these basic questions have not been given so far.

This study attempts to explain the counter-intuitive background physics by the use of a physically sound equivalent circuit of the realistic negative capacitor. This model is able to explain the physical origin of the instability and all other counter-intuitive effects observed so far. The model is verified by measurements on a specially designed laboratory prototype, both in the time domain and the frequency domain.

Equivalent circuit of negative capacitor – theoretical investigation

In order to investigate the basic physics of negative capacitor, it is very convenient to construct an equivalent circuit. One way of doing this could be to study the standard NIC designs [3,5] and work out the appropriate equivalent circuits. Obviously, the different designs would yield the different equivalent circuits. In principle, it should be possible to use standard circuit-theory transformations and recast all these circuits into a "generic" equivalent circuit. However, it is difficult to identify the design details that can be neglected in order to keep the equivalent circuit physically sound and, at the same time, as simple as possible.

Therefore, we decided to use physical (bottom-up) approach that starts from the basic equations (1) and (2). Rearranging (2) in a way that uses a positive

capacitor C_p, one gets

$$i_n(t) = -|C_n|\frac{\partial v(t)}{\partial t} = |C_n|\frac{\partial[-v(t)]}{\partial t} = C_p\frac{\partial[-v(t)]}{\partial t}. \quad (5)$$

The rightmost part of (5) clearly shows that the negative capacitor C_n can be thought of as a positive capacitor C_p with a flipped sign of the voltage ($v(t) \rightarrow -v(t)$). Thus, the polarity of the "internal" voltage that excites a capacitor should somehow be reversed. A simple way of achieving this sign reversal is sketched in Figure 4(a).

Here, a positive capacitor C_p is connected in series with a voltage source $v_0(t)$ that is controlled by the input signal $v(t)$. The amplitude of $v_0(t)$ is chosen to be twice the amplitude of the input signal ($v_0(t) = 2v(t)$). Since the voltage drop across the capacitor C_p is negative ($v_c(t) = v(t) - 2v(t) = -v(t)$), the net current $i(t)$ is also negative. Thus, the current $i(t)$ flows outward of the negative capacitor (it is actually the output current of a controlled source). In practice, the controlled voltage source ($v_0(t) = 2v(t)$) can be implemented by an amplifier with (voltage) gain $A = +2$ (Figure 4(a)).

The effect of a capacitance sign flip (assuming simple monochromatic signal) is explained in the phasor diagram in Figure 4(b). The phasor of the current (I) leads the associated voltage across the capacitor (V_c) by 90°, which is a familiar behaviour. At the same time, the phasor of the current (I) does lag the phasor of the input voltage (V) by 90°. This phase lag (looking from the input terminals) clearly explains the existence of a negative capacitance C_n.

The simple model in Figure 4(a) can explain the occurrence of instability. Let us go back to the example of an initially charged negative capacitor connected instantaneously to the resistor R (Figure 2). In the equivalent circuit (Figure 4(a)), it means that there is some initial voltage V_0 that suddenly occurs at the input of the amplifier. This initial voltage will appear at the output of the amplifier, as well (however, its level will be doubled due to the gain of the amplifier). Output (amplified) voltage will be fed back again to the input, then amplified again, fed back to the input, etc. Thus, the voltage will continually grow causing the instability (of course, in practice, the maximal voltage will be limited by the DC power supply of the amplifier). A very important situation occurs in the case of an "isolated" negative capacitor (a negative capacitor without any other external elements connected to it). Theoretically, if the input of the amplifier in Figure 4(a) is left open, both the input and the output voltages will be zero and the circuit should be stable. However, in reality, there is always some noise present at the input of the amplifier. Thus, the same effect of consequent round-trip amplifications that cause signal grow will occur again (the only difference from the previous example is that the initial signal is now of stochastic nature). Obviously, this process resembles the behaviour of an ordinary oscillator and leads to self-oscillations (one should be aware that any signal waveform is allowed in this idealized case with infinite-bandwidth amplifier). This effect clearly explains the physical origin of the instability of an "isolated" negative capacitor observed in previous experimental studies [1,2,7,8].

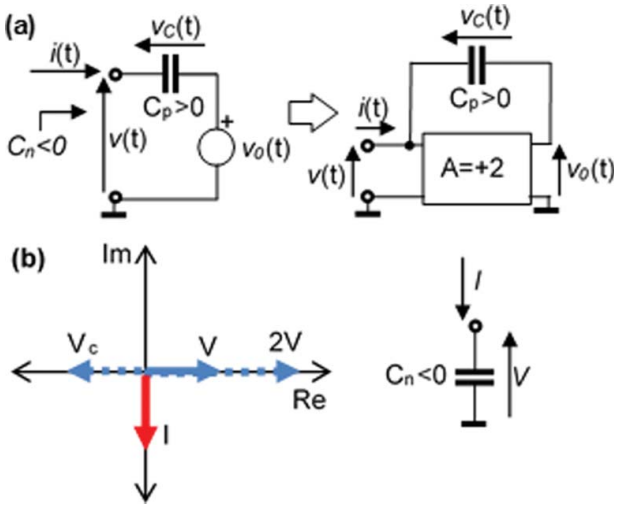

Figure 4. (a) Evolution of a model of negative capacitor based on the controlled voltage source (voltage amplifier). (b) Phasor diagram of an ideal negative capacitor.

Previous studies [7,8] also showed that a parallel combination of a negative capacitor (C_n) and some external positive capacitor (C_{pext}) (Figure 5(a)) is stable, providing that $C_{pext} > |C_n|$.

Taking advantage of the equivalent circuit from Figure 4(a), one realizes that a parallel combination of C_{pext} and C_n actually means that the external capacitor C_{pext} is connected to the input terminals of the amplifier input Figure 5(b)). Here, the external capacitor C_{pext}, together with a feedback capacitor C_p, forms a capacitive voltage divider. This divider determines a level of amplified noise fed back to the input of the amplifier. The oscillations cannot be self-sustained if the noise level at the amplifier input is less than half of the noise level at the output of the amplifier (due to $A = +2$). Therefore, the step-down ratio of a capacitive divider ($C_p/(C_p+C_{pext})$) should not exceed 1:2, which

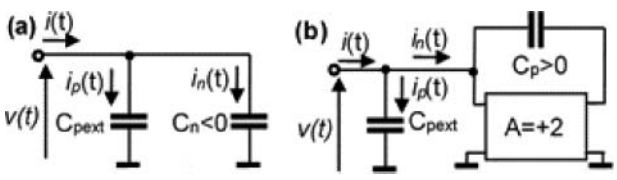

Figure 5. (a) Connection of a positive (C_{pext}) and a negative (C_n) capacitance. C_{pext} is an external (stabilizing) capacitor. (b) Connection of a positive (C_{pext}) and a negative (C_n) capacitance model. C_{pext} is an external (stabilizing) capacitor.

means that the system will be stable only if $C_{pext} > |C_n|$. Again, this intuitive conclusion is in perfect agreement with previous studies [7–9]. Equally important, the circuit with the external capacitor C_{pext} is (in principle) identical to a basic circuit in non-Foster metamaterials based on a transmission line loaded with negative capacitors [1,2] (Figure 3). So, it also explains the background physics of a capacitance decrease effect, formally given by (4). One should be aware that, in this scenario, there are actually two currents flowing simultaneously into the external capacitor (C_{pext} in Figure 5 (a)). The first current ($i_p(t)$) is caused by an external generator ($v(t)$) while the second current $i_n(t)$ actually flows from the output of the amplifier (thus, a negative capacitor again acts as an additional source). Therefore, the current that flows into the positive capacitor C_{pext} is higher than the current which would flow into it if the negative capacitor were not present. This higher current brings more charge per unit of time causing faster charging/discharging. This effect can be interpreted as the decrease of the overall capacitance described by (4).

The above discussion has shown that the initial model in Figure 4(a) clearly explains many of the counter-intuitive physical effects reported in the literature [1–3,7–9]. However, one should be aware that this model employs an unrealistic amplifier with a constant gain across infinite bandwidth. Due to this, the modelled negative capacitance is entirely dispersionless, which is not consistent with the principle of causality [5,17]. Of course, it would be very convenient to overcome this drawback, i.e. to include causality in the model. The improved (causal) model should be able to correctly and accurately predict all physical effects of the negative capacitor.

Towards this end, one starts from a fact that every realistic amplifier used in a negative capacitor always introduces some delay. At one fixed frequency, the delay can be described by a phase shift ϕ between the output and the input signal (Figure 6).

Here, the phasor of the current flowing through the capacitor (I) lags the phasor of the input voltage (V) by an angle that is greater than 90°. So, the input current has both a reactive (capacitive) component (I_{Cn}) and a lossy (resistive) component (I_{Gn}). Thus, the realistic negative capacitor always behaves as a parallel combination of the negative capacitance (C_n) and the negative conductance (G_n). This explains why all the experimental results published so far revealed, apart from the negative capacitance, existence of (unwanted) negative conductance [1–3,7,8,18]. The next step is to analytically describe the variation of the phase shift ϕ with frequency. The phase variation (and accompanied gain variation) can be modelled by a multi-pole transfer function of the used amplifier (in Laplace s-domain):

$$A(s) = \frac{A_0}{\prod_{i=1}^{i=n}\left(1 + \frac{s_i}{\omega_i}\right)}. \tag{6}$$

Here, A_0 stands for the zero-frequency gain, n is the number of poles and ω_i is the angular frequency of i-th pole s_i. We found that a three-pole model ($n = 3$) is sufficient for an accurate modelling of practical negative capacitors. Equation (6) assures required causality of the modelled negative capacitor. Indeed, when the frequency ω approaches infinity, the gain $A(s)$ (and, therefore, the voltage of the controlled source as depicted in Figure 4(a)) approaches zero. Consequently, the equivalent capacitance becomes a positive number that approaches C_p. Visualization of this dispersive behaviour is possible using the phasor diagram (Figure 6). The phase shift ϕ increases with an increase in frequency (since the delay time becomes a larger part of a period of the signal). Hence, the phasor I rotates clockwise and its length becomes shorter (due to gain decrease with the frequency), as indicated by the dashed curve in Figure 6. This effect, in turn, increases I_{Gn} and decreases I_{Cn} (thus, it increases the generated negative conductance and decreases the negative capacitance). At some particular frequency, reactive component of the input current (I_{Cn}) will become zero and the negative capacitance effect ceases. Further increase of the frequency moves the phasor I from the third and across the second quadrant of the complex plane. Thus, the equivalent input impedance becomes a parallel combination of a positive capacitance and a negative conductance. Finally (at the frequency of the third pole), the phasor I lies on the positive imaginary axis and the input admittance becomes a pure positive capacitance (C_p). Going back to the intriguing broadband superluminal effects in non-Foster ENZ metamaterials [2] (Figure 3), they actually rely on an inevitable dispersion of a negative capacitor. Only the frequency components of the signal that lie within the operating band of the non-Foster negative capacitor travel with the superluminal velocity. However, the spectrum of a signal will never be finite in the transient state (the switching-on phase of the generator). So, there is

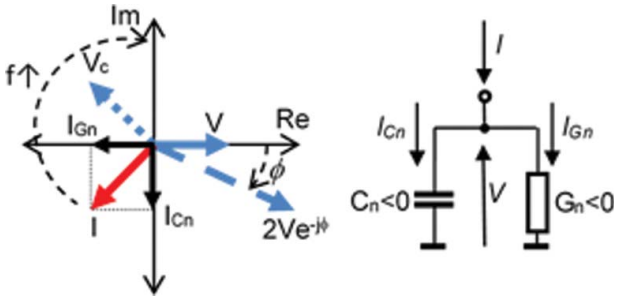

Figure 6. Phasor diagram of a realistic negative capacitor. Clockwise rotation of a current phasor with the frequency increase is indicated.

always a fraction of energy (however small it is) that lies outside the operating band of a negative capacitor. This fraction of energy travels with the speed of light, preserving the causality. In other words, with the increase of the frequency, the effective permittivity approaches +1 and the velocity approaches the speed of light. Of course, this behaviour is perfectly consistent with causality. Therefore, the proposed equivalent circuit of a negative capacitor, based on a dispersive controlled voltage source (Figure 4(a) and Equation (6)), is indeed physically sound.

One may argue that the proposed model is nothing more than one of the standard variants of NIC. However, this is not true. Figure 4 represents the simplest circuit-theory equivalent circuit, directly inferred from the basic definitions of negative capacitance, with required corrections that assure compatibility with causality. It actually shows that a negative capacitor cannot be thought of a simple circuit element but rather as an active control system. All practical designs can be reduced to the equivalent circuit from Figure 4. Finally, the most important property of the proposed equivalent circuit is that it correctly predicts all physical phenomena previously observed in networks with negative capacitor.

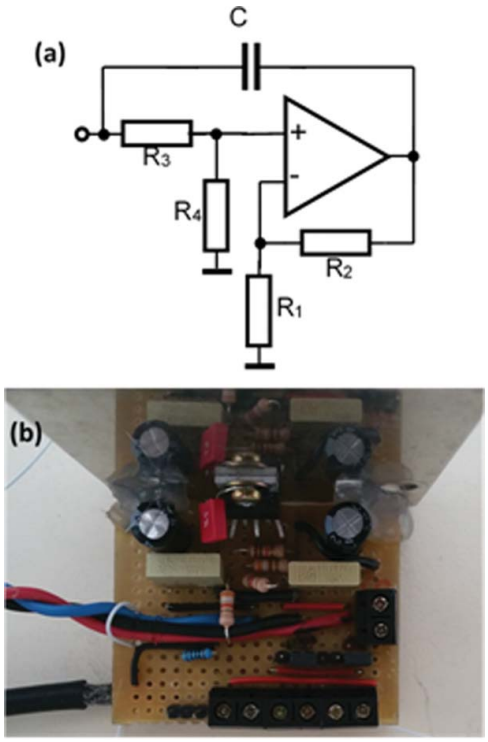

Figure 7. (a) Negative capacitor demonstrator (C = 1 μF, $R1$ = 390 Ω, $R2$ = 3900 Ω, $R3$ = 4500 Ω, $R4$ = 1000 Ω), LM1875 amplifier (supply voltage ±15 V). $R1$–$R4$ form an amplifier with $A_0 = 2$ (associated poles are: $s_{1,2} = \pm 1.29 \times 10^6 + j4.73 \times 10^5$ rad, $s_3 = 0 + j1.03 \times 10^7$ rad). (b) Photograph of the prototype.

Equivalent circuit of negative capacitor – experimental investigation

In the experimental part of this study, we prototyped a simple negative capacitor demonstrator (Figure 7). The purpose of this demonstrator was twofold: to verify the explanation of the counter-intuitive physics and to test the correctness of the dispersive multi-pole model.

Although the majority of proposed applications of the negative capacitors are in the radio-frequency (RF) band [1–3,7–9], this regime is inconvenient for direct time-domain measurements (the value of the generated negative capacitance is usually in the same order of magnitude as the input capacitance of the oscilloscope probes (a few pF), which affects the measurements). Thus, the demonstrator (Figure 7(a)) was designed to operate at very low-frequencies (up to 25 kHz). It was based on the integrated audio amplifier LM1875, arranged into the circuit that is a straightforward hardware replica of the basic idea from Figure 4(a) (Figure 7(a)). Due to the use of an integrated amplifier that can supply high output current (up to 3 A), it was possible to generate a very large value of the negative capacitance (−1.2 μF) [18]. This value is several orders of magnitude higher than the input capacitance of an oscilloscope, assuring simple and reliable time-domain measurements. A photograph of the assembled prototype can be seen in Figure 7(b).

In the first experiment, the basic stability constraints of a negative capacitor were checked by time-domain measurements. Several different parallel combinations of a positive capacitor and the negative capacitor (i.e. the LM1875-based demonstrator) were investigated (Figure 5(a)). The voltage and current waveforms were monitored by a digital oscilloscope (Tektronix TDS 2024B) and the current probe (Tektronix TM502A with AM503 amplifier). No voltages or currents were observed in the $C_{pext}C_n$ mesh if $C_{pext} > |C_n|$. On the contrary, if $C_{pext} < |C_n|$, the circuit was unstable (the negative capacitor was oscillating). Furthermore, the stand-alone demonstrator (isolated negative capacitor) was unstable. These results are in perfect agreement with the presented theory. Since the initial testing verified the correctness of stability requirements, all subsequent experiments used parallel combination of a positive and negative capacitors ($C_{pext} > |C_n|$).

In the second experiment, the expected existence of a non-Foster negative capacitance was verified by measurements on a simple $RC_{pext}C_n$ test network (Figure 8(a)).

The network was excited by CFG600 Tektronix function generator (adjusted to 2.4 kHz sinusoidal signal) and the voltage and current waveforms were monitored again. The measured waveforms (Figure 8(b)) revealed a familiar positive phase shift of +90° between current and voltage at the positive capacitor (thus, the

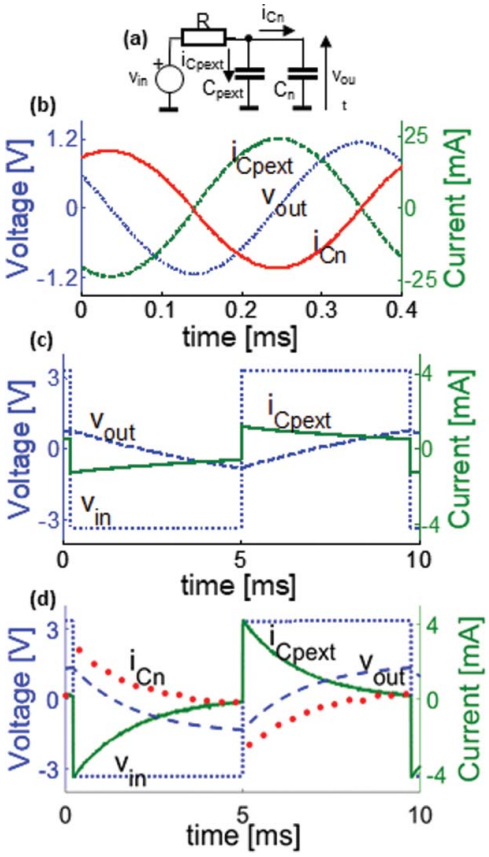

Figure 8. (a) Setup for investigation of the effect of capacitance decrease (R = 3900 Ω, C_{pext} = +2 μF, C_n = −1.2 μF). (b) Measured currents through the positive capacitor (dashed) and through the negative capacitor (solid), compared with the input sinusoidal voltage (dotted). (c) Measured current flowing into the positive capacitor C_{pext} (solid) and voltages at the input (dotted) and at the output (dashed) of the integrator without the negative capacitor. (d) Measured current flowing into the external positive capacitor C_{pext} (solid), current flowing into the negative capacitor C_n (full circles), input voltage (dotted) and output voltage (dashed) of the integrator with the negative capacitor.

current led the voltage). However, the phase shift between current and voltage at the negative capacitor was found to be negative (−90°), and thus the voltage led the current. The effect of voltage lead was observed for all the frequencies in the 1–25 kHz band. Associated susceptance (a ratio of current and voltage magnitudes) decreased monotonically across the same band. This shows $\partial B/\partial\omega < 0$, which is a direct proof of non-Foster behaviour, i.e. the proof of generated negative capacitance. In addition, it is clearly seen that there is 180° phase difference between the current i_{cpext} and the current i_{cn}. In other words, the current i_{cn} actually flows out from the negative capacitor, which is consistent with (2) and Figure 1.

The third experiment dealt with a counter-intuitive effect of overall capacitance decrease [1,2] (4). This time, the $RC_{pext}C_n$ test network (Figure 8(a)) was driven by a signal with a square waveform of frequency 105 Hz. In the first step, the negative capacitor was disconnected from the network leaving an ordinary, positive RC circuit (an integrator). Measured waveforms (Figure 8(c)) revealed familiar charging and discharging of the positive capacitor. However, the presence of the negative capacitor fundamentally changed this situation (Figure 8(d)). Here, the output voltage change is faster. Again, it happens due to the fact that the current $i_{cn} < 0$. Thus, this current actually flows out from the negative capacitor (because the negative capacitor behaves like a source; see (2)). On the contrary, the current i_{cpext} flows into the positive capacitor. Due to this difference in directions, the current that flows into the positive capacitor (i_{cpext}) is higher than the current which would flow if there were no negative capacitor (a case shown in Figure 8(c)). Thus, the negative capacitor is indeed a source that "assists" in charging and discharging of a positive capacitor and it decreases the effective capacitance. Again, this effect occurred in the whole 1–25 kHz band.

In the last part of the experimental investigation, the three-pole model was extracted from the LM1875 manufacturer data. Then, equivalent input capacitance and conductance (Figures 9(a,b)) were calculated using presented theory (Figure 6 and (6)). In addition, the input capacitance and conductance were simulated using the Ansoft ADS^{TM} circuit-theory simulator and the manufacturer's SPICE model of the LM1875 amplifier. These two sets of data are compared in Figure 9(a,b).

It can be seen that the three-pole model matches simulation very closely, both qualitatively and numerically. There is a "flat" region with nearly constant negative capacitance and it extends approximately to the frequency of the first pole. At that frequency, the phase shift is not any more negligible and it causes the occurrence of the negative conductance. At even higher frequencies, negative capacitance effect ceases and (at the frequency of the third pole) the equivalent capacitance is a positive number that approaches C_{pext}.

Finally, the equivalent input capacitance and conductance of the demonstrator were measured in the frequency domain using HP4294A impedance analyser and the results are shown in Figure 9(c,d). The measurement used previously developed de-embedding procedure [1]. Briefly, an additional capacitor (2 μF) was connected in parallel to the input terminals of a demonstrator, ensuring stability. Then, the overall capacitance and conductance of a parallel combination was measured and the (also measured) capacitance of the stabilizing capacitor was subtracted. It can be seen that the obtained results (Figure 9(c,d)) qualitatively match both the three-pole theory and the simulations. Furthermore, the measurements numerically match the theory and simulations extremely well for most of the frequencies. However, measured values appear to be up to three times larger than those from the theory

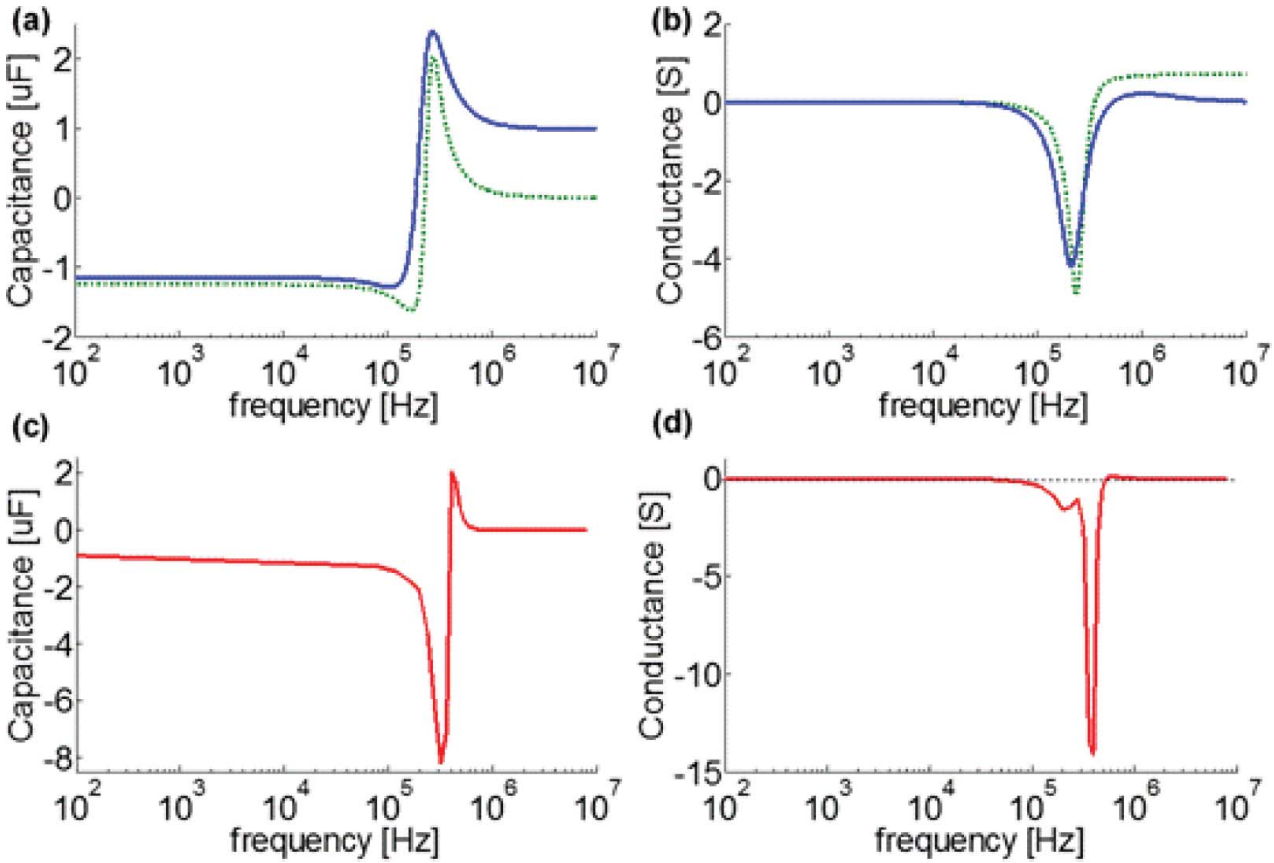

Figure 9. (a) Theoretical capacitance of the demonstrator. Solid: three-pole theory. Dashed: circuit-theory (SPICE-based) simulations. (b) Theoretical conductance of the demonstrator. Solid: three-pole theory. Dashed: circuit-theory simulations. (c) Measured capacitance of the demonstrator. (d) Measured conductance of the demonstrator.

and simulations, in the vicinity of the 300 kHz frequency. Additional investigation revealed that this discrepancy occurred due to pure technological problems, i.e. due the parasitic inductance of 1 μF capacitor used in the demonstrator (the capacitor C_p in Figure 4(a)). The self-resonant-frequency of the used capacitor was found to be at the frequency of 300 kHz (this is a rather typical value for standard commercial capacitors, capacitance of which lies in μF range). In the vicinity of this self-resonant frequency, the capacitor actually behaved as a parallel *LC* circuit, which caused the above apparent inconsistency.

Conclusions

It has been shown that (widely used) approximation of a realistic non-Foster negative capacitor with ideal dispersionless model is fundamentally incorrect. Ideal negative capacitor is not causal and, therefore, not compatible with basic physics. Due to this, a physically sound equivalent circuit of a realistic negative capacitor has been developed and verified, both numerically and experimentally. The model is based on a dispersive controlled voltage source. Presented analysis and experiments show that this model accurately predicts instability and all other previously reported counter-intuitive physical phenomena. Therefore, presented model may be very useful in design of future devices based on negative capacitors.

Acknowledgments

The authors thank Dr Tihomir Marjanović for help in the measurements and Mr Ante Orsulic for assembling the prototype.

Disclosure statement

No potential conflict of interest was reported by the authors.

Funding

This work is supported by the European Office of Aerospace Research and Development [contract number FA9550-15-1-0120]; the Unity through Knowledge Fund (UKF) [contract number 09/13]; and European Social Fund [contract number HR.3.2.01-0309].

References

[1] Hrabar S, Krois I, Bonić I, et al. Negative capacitor paves the way to ultra-broadband metamaterials. Appl Phys Lett. 2011;99:25403, 254103–1, 254103–4.
[2] Hrabar S, Krois I, Bonic I, et al. Ultra-broadband simultaneous superluminal phase and group velocities

in non-Foster epsilon-near-zero metamaterial. Appl Phys Lett. 2013;102:054108, 054108–1, 054108–5.
[3] Perry AK. Broadband antenna systems realized from active circuit conjugate impedance matching. AD-769 800. Springfield (VA): National Technical Information Service; 1973. Available from: http://www.dtic.mil/dtic/tr/fulltext/u2/769800.pdf
[4] Pozar DM. Microwave engineering. Willey; 1998.
[5] Nedlin G. Energy in lossless and low-loss networks, and Foster's reactance theorem. IEEE Trans Circuits Syst. 1989;36:561–567.
[6] Linvill JG. Transistor negative impedance converters. Proc IRE. 1953;41:725–729.
[7] Stearns SD. Non-Foster circuits and stability theory. Proceedings of IEEE APS-URSI, Spokane (WA). New York (NY): IEEE; 2011. p. 1942–1945.
[8] Ugarte-Munoz E, Hrabar S, Segovia-Vargas D, et al. Stability of non-Foster reactive elements for use in active metamaterials and antennas. IEEE Trans Antennas Propag. 2012;60:3490–3494.
[9] Tretyakov S, Maslovski S. Veselago materials: what is possible and impossible about the dispersion of the constitutive parameters. IEEE Antennas Propag Mag. 2007;49:37–43.
[10] Rengarajan SR, White CR. Stability analysis of superluminal waveguides periodically loaded with non-Foster circuits. Antennas Wirel Propag Lett. 2013;12:1303–1306.
[11] Karlsson K, Carlsson J. Non-Foster networks for improvement of radiation efficiency and effective diversity gain of a multi-port antenna. Proceedings of European Conference on Antennas and Propagation (EuCAP), Barcelona, Spain. New York (NY): IEEE; 2010. p. 1–4.
[12] Zhang F, Sun B, He K, et al. Study and design of a broadband monopole antenna using non-Foster circuits. Proceedings of the 9th International Symposium on Antennas, Propagation and EM Theory, Guangzhou, China. New York (NY): IEEE; 2010. p. 60–63.
[13] Ledezma LM. Doherty power amplifier with lumped non-Foster impedance inverter. 2015 Texas Symposium on Wireless and Microwave Circuits and Systems (WMCS), Waco (TX). New York (NY): IEEE; 2015. p. 1–4.
[14] Ford KL. Oblique incidence analysis of a Salisbury screen employing a non-Foster matching technique. Proceedings of the Loughborough Antennas Propagation Conference, Loughborough, UK. New York (NY): IEEE; 2013. p. 510–513.
[15] Lundry WR. Negative impedance circuits-some basic relations and limitations. IRE Trans Circuit Theory. 1957;4:132–139.
[16] Stearns SD. Counterintuitive aspects of non-Foster networks. Presentation in Adelphi Antenna Workshop on Electrically Small Antennas, New York (NY); 2010.
[17] Landau LD, Lifshitz EM, Pitaevskii LP. Electrodynamics of continuous media. Oxford: Butterworth Heinemann; 2002.
[18] Okorn B, Hrabar S, Krois I. Investigation of basic physics of non-Foster negative capacitance in time domain. Proceedings of ELMAR, Zadar, Croatia. New York (NY): IEEE; 2011. p. 373–376.